The Plant Cell, Vol. 23: 4382–4393, December 2011, www.plantcell.org

GIGAS CELL1, a Novel Negative Regulator of the Anaphase-Promoting Complex/Cyclosome, Is Required for Proper Mitotic Progression and Cell Fate Determination in *Arabidopsis* [W]

Eriko Iwata,[a] Saki Ikeda,[a] Sachihiro Matsunaga,[b] Mariko Kurata,[a] Yasushi Yoshioka,[c] Marie-Claire Criqui,[d] Pascal Genschik,[d] and Masaki Ito[a,1]

[a] Graduate School of Bioagricultural Sciences, Nagoya University, Chikusa, Nagoya 464-8601, Japan
[b] Department of Applied Biological Science, Tokyo University of Science, Noda Chiba 278-8510, Japan
[c] Division of Biological Science, Graduate School of Science, Nagoya University, Chikusa-ku, Nagoya 464-8602, Japan
[d] Institut de Biologie Moléculaire des Plantes, Centre National de la Recherche Scientifique, Unité Propre de Recherche 2357, 67084 Strasbourg, France

Increased cellular ploidy is widespread during developmental processes of multicellular organisms, especially in plants. Elevated ploidy levels are typically achieved either by endoreplication or endomitosis, which are often regarded as modified cell cycles that lack an M phase either entirely or partially. We identified *GIGAS CELL1* (*GIG1*)/*OMISSION OF SECOND DIVISION1* (*OSD1*) and established that mutation of this gene triggered ectopic endomitosis. On the other hand, it has been reported that a paralog of *GIG1*/*OSD1*, *UV-INSENSITIVE4* (*UVI4*), negatively regulates endoreplication onset in *Arabidopsis thaliana*. We showed that *GIG1*/*OSD1* and *UVI4* encode novel plant-specific inhibitors of the anaphase-promoting complex/cyclosome (APC/C) ubiquitin ligase. These proteins physically interact with APC/C activators, CDC20/FZY and CDH1/FZR, in yeast two-hybrid assays. Overexpression of CDC20.1 and CCS52B/FZR3 differentially promoted ectopic endomitosis in *gig1*/*osd1* and premature occurrence of endoreplication in *uvi4*. Our data suggest that GIG1/OSD1 and UVI4 may prevent an unscheduled increase in cellular ploidy by preferentially inhibiting APC/C^{CDC20} and APC/C^{FZR}, respectively. Generation of cells with a mixed identity in *gig1*/*osd1* further suggested that the APC/C may have an unexpected role for cell fate determination in addition to its role for proper mitotic progression.

INTRODUCTION

In multicellular organisms, organ sizes are determined by cell division and cell expansion. The former is conducted by continuous progression of the mitotic cell cycle, whereas the latter is partly achieved by atypical modes of the cell cycle that lead to elevated cellular ploidy (Edgar and Orr-Weaver, 2001). Typically, an increase in ploidy levels is executed by two different strategies, endoreplication and endomitosis, where cells replicate their chromosomes without division (see Supplemental Figure 1 online). Endoreplication, which lacks the entire processes of mitosis, does not affect the number of chromosomes but generates polytene chromosome (Edgar and Orr-Weaver, 2001; Lee et al., 2009). On the other hand, in endomitosis, cells enter but do not complete mitosis, most typically proceeding through anaphase but lacking nuclear division and cytokinesis (D'Amato, 1984; Lee et al., 2009). In contrast with endoreplication, endomitosis causes doubling of the chromosome number, yielding cells with a single polyploid nucleus. Endoreplication is widespread especially in plants and is associated with cessation of cell division and onset of cell differentiation during developmental processes in various organs (Beemster et al., 2005; Breuer et al., 2010, De Veylder et al., 2011). Less attention has been paid to endomitosis, but it is also known to occur in various plant species, including *Arabidopsis thaliana* (Weiss and Maluszynska, 2001), most frequently during development in the tapetum and endosperm (Nagl, 1978; D'Amato, 1984).

Onset of endoreplication typically requires inhibition of mitotic cyclin-dependent kinase (CDK) activities (Lilly and Duronio, 2005; Inzé and De Veylder, 2006), which is often associated with the degradation of mitotic cyclins by the anaphase-promoting complex/cyclosome (APC/C) in insects (Narbonne-Reveau et al., 2008; Zielke et al., 2008) and plants (Cebolla et al., 1999; Larson-Rabin et al., 2009; Eloy et al., 2011). APC/C is a multisubunit protein complex acting as an E3 ubiquitin ligase (Peters, 2006) and is responsible for the transition of key mitotic processes by targeted degradation of numerous cell cycle proteins (Peters, 2006; Marrocco et al., 2010). In contrast with endoreplication, little is known about the mechanisms underlying endomitosis, which, however, may be triggered by the depletion of mitotic cyclins mediated by the APC/C (Zhang et al., 1998).

[1] Address correspondence to masakito@agr.nagoya-u.ac.jp.
The author responsible for distribution of materials integral to the findings presented in this article in accordance with the policy described in the Instructions for Authors (www.plantcell.org) is: Masaki Ito (masakito@agr.nagoya-u.ac.jp).
[W] Online version contains Web-only data.
www.plantcell.org/cgi/doi/10.1105/tpc.111.092049

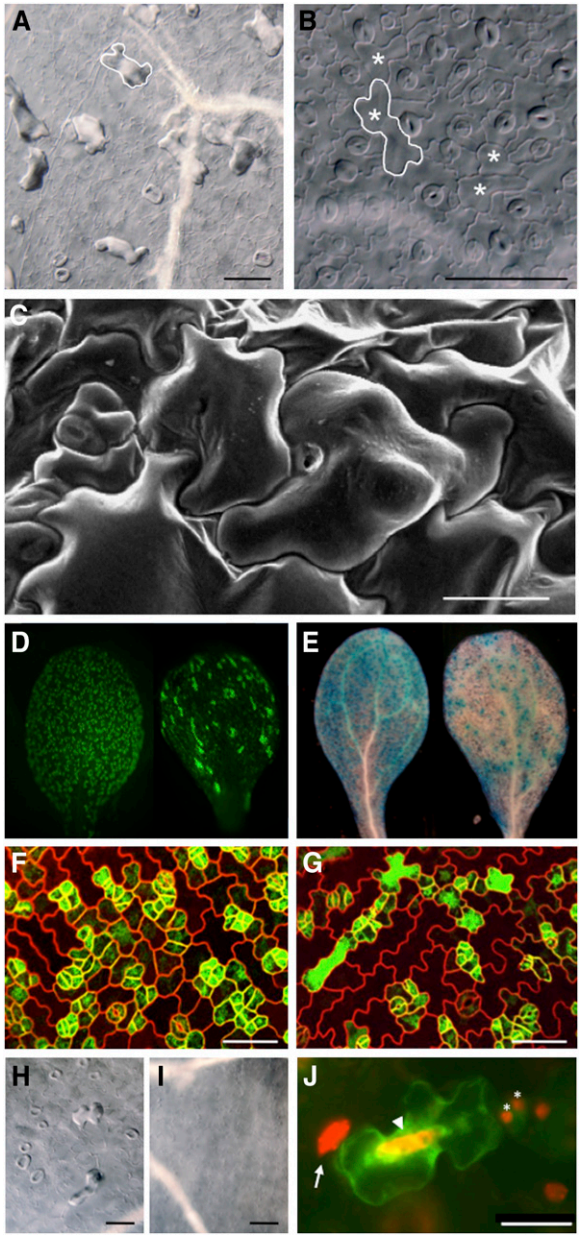

Figure 1. Loss of *GIG1* Causes the Occurrence of Giant Cells with Guard Cell–Like Characteristics.

(A) and **(B)** Giant guard cell–like cells in cotyledons **(A)** and leaves **(B)** in *gig1-2* seedlings observed by DIC microcopy. These cells are herein called *gigas* cells. Outline of an example of a *gigas* cell is marked by the white solid line in each image. Asterisks indicate *gigas* cells in **(B)**.

(C) *Gigas* cells are occasionally accompanied by structures similar to stomatal pores as observed by scanning electron microscopy.

(D) and **(E)** Expression of guard cell–specific markers, E1728 **(D)** and KAT1:GUS **(E)**, in *gigas* cells. Wild-type cotyledon, left; *gig1-2* cotyledon, right.

(F) and **(G)** Expression of TMM:GUS-GFP in wild-type **(F)** and *gig1-1 myb3r4* **(G)** cotyledons. Cell outlines were visualized by counterstaining with FM4-64 (shown in red).

(H) and **(I)** Mutation in *spch* eliminates not only guard cells but also *gigas* cells in cotyledons of *gig1-1 myb3r4* seedlings. Cleared cotyledons from double *gig1-1 myb3r4* mutants **(H)** and triple *gig1-1 myb3r4 spch* mutants **(I)** were observed by DIC.

(J) Enlarged nuclei in *gigas* cells. Cotyledons of *gig1-1 myb3r4* seedlings were stained with DAPI (shown in red). A *gigas* cell expressing TMM:GUS-GFP (shown in green) contains an enlarged nucleus (arrowhead) in comparison with dividing stomatal lineage cells (asterisks). Note that the nuclear size of the *gigas* cell is equivalent to that of the adjacent endoreplicated pavement cell (arrow).

Bars = 50 μm in **(A)** to **(C)** and **(F)** to **(I)** and 20 μm in **(J)**.

APC/C activity is generally regulated by both activator and inhibitor proteins (Peters, 2006). APC/C activators, CELL DIVISION CYCLE20 (CDC20)/FIZZY (FZY) and CDC20 HOMOLOG1 (CDH1)/FZY-RELATED (FZR), are evolutionarily conserved, and their binding to APC/C is critical for its ubiquitination activity (Pesin and Orr-Weaver, 2008). *Arabidopsis* has counterparts of both types of activators, of which CELL CYCLE SWITCH 52A2 (CCS52A2)/FZR1 and CCS52A1/FZR2 are known to positively regulate the onset of endoreplication in different developmental contexts (Lammens et al., 2008; Larson-Rabin et al., 2009). However, there is no *Arabidopsis* gene that corresponds to the APC/C inhibitors found in metazoa and yeasts, and it remained unclear if plants have such inhibitor proteins at all. Here, we report that *GIGAS CELL1* (*GIG1*) and *UV-INSENSITIVE4* (*UVI4*), a paralog of *GIG1*, may encode novel plant-specific inhibitors of APC/C. GIG1 may prevent the ectopic occurrence of endomitosis by inhibiting CDC20-dependent APC/C (APC/C^{CDC20}), while UVI4 may have negative effects on endoreplication onset by inhibiting FZR-dependent APC/C (APC/C^{FZR}) activity. Strikingly, our results suggest that GIG1 may be required not only for proper mitotic progression but also for normal cell fate determination during stomatal development.

RESULTS

Loss of *GIG1* Generates Giant Guard Cells

The two allelic recessive mutants *gig1-1* and *gig1-2* were obtained in a forward genetic screen to identify enhancers of the *myb3r4* mutant phenotype (Haga et al., 2011). MYB3R4 belongs to the Myb family of transcriptional regulators that positively regulate mitotic progression in *Arabidopsis*. These mutants displayed giant cells, which were also observed in *gig1* plants without the *myb3r4* mutation, although this phenotype was strongly enhanced when *MYB3R4* was simultaneously mutated (see Supplemental Figure 2 online). The giant cells in *gig1* cotyledons, herein designated as *gigas* cells, showed guard cell–like appearance in differential interference contrast (DIC) images, suggesting that their cell walls may be biochemically similar to each other (Figures 1A and 1B). These cells showed some other guard cell–like characteristics, including possession of structures similar to stomatal pores (Figure 1C) and expression of guard cell–specific markers, E994, E1728, and KAT1:β-glucuronidase (GUS) (Figures 1D and 1E; see Supplemental Figure 3 online) (Ohashi-Ito and Bergmann, 2006; Pillitteri et al., 2007). We also showed that generation of *gigas* cells is

associated with TOO MANY MOUTHS (TMM):green fluorescent protein (GFP) expression, a marker for stomatal precursor cells (Nadeau and Sack, 2002) (Figures 1F and 1G), and requires *SPEECHLESS* (*SPCH*) function, which is essential for stomatal development (Pillitteri et al., 2007) (cf. Figures 1H and 1I). These results suggest that *gigas* cells may have a guard cell–like identity, which may be generated through a similar developmental pathway that generates stomata. However, the *gigas* cells are more similar to jigsaw puzzle–shaped pavement cells in terms of size and morphology and are not paired, in contrast with guard cells in normal stomata. Furthermore, their nuclei are larger than those in normal guard cells and their precursors and are equivalent in size to endoreplicated nuclei in pavement cells (Figure 1J; see Supplemental Figure 4 online).

In addition to the *gigas* cells, the *gig1* cotyledons have two other types of abnormal cells: large guard cells and round cells (see Supplemental Figure 5 online). The former is characterized by abnormally enlarged guard cells, a pair of which forms normal-shaped giant stomata. The latter is reminiscent of single-celled stomata, which are typically generated when guard mother cells fail to undergo cytokinesis or are arrested at the G2 phase, but achieved differentiation into guard cells (Falbel et al., 2003; Boudolf et al., 2004). This notion is consistent with our observation that guard cell–specific markers, E994 and KAT1:GUS, were expressed in the round cells (see Supplemental Figures 3 and 5 online).

All of these abnormal cell types were observed both in *gig1-1* and *gig1-2*, irrespective of the presence of the *myb3r4* mutation. There were no qualitative differences in epidermal phenotypes among the mutant combinations, which only affect the frequency of such abnormal cells. In the following experiments, we used both *gig1-1* and *gig1-2* alleles, which were, in some cases, combined with the *myb3r4* mutation, especially when the weak *gig1-1* allele was used.

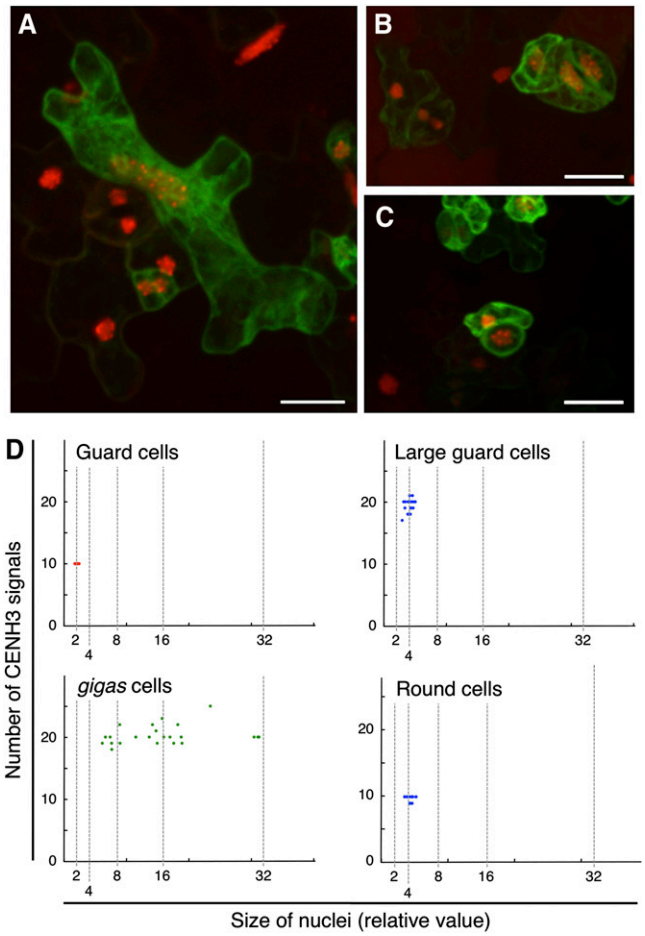

Figure 2. Occurrence of Cellular Polyploidy in the *gig1-1 myb3r4* Epidermis.

(A) to **(C)** Abnormal cells in the *gig1-1 myb3r4* epidermis expressing kinetochore marker tdTomato-CENH3. All three types of abnormal cells, *gigas* cells **(A)**, large guard cells **(B)**, and round cells **(C)**, expressed a marker of stomatal lineage cells, TMM:GUS-GFP (shown in green), and contained enlarged nuclei, as visualized by tdTomato-CENH3 (shown in red). Fluorescence of tdTomato-CENH3 was observed in kinetochores as bright dots and in whole nuclei as weak and uniform signals. Bars = 20 μm.
(D) Ploidy maps representing nuclear sizes and numbers of chromosomes in normal guard cells and abnormal cells in the epidermis of *gig1-1 myb3r4* seedlings. Number of chromosomes was determined by counting bright dots of tdTomato-CENH3 signals within each nucleus, whereas weak and uniform fluorescence of tdTomato-CENH3 in whole nuclei was used for quantification of nuclear sizes.

Occurrence of Endomitosis in *gig1* Cotyledons

All three types of abnormal cells in *gig1* cotyledons (*gigas* cells, large guard cells, and round cells) contained enlarged nuclei in comparison with those of wild-type guard cells (Figure 1J; see Supplemental Figure 5 online), suggesting increased ploidy levels of these cells. To quantitatively analyze the polyploidy, we estimated nuclear DNA content by measuring relative nuclear sizes and determined the number of chromosomes in each nucleus using a kinetochore-specific marker, tdTomato-CENH3 (Figures 2A to 2D) (Kurihara et al., 2008). The normal guard cells, containing 2C nuclei with relative nuclear sizes of 2.0, showed 10 spots marked by tdTomato-CENH3, which are equivalent to diploid chromosome number (2*n*) of *Arabidopsis*. By contrast, the round cells exhibited nuclei with relative sizes of around 4.0 containing 10 chromosomes, which can be explained by G2 cell cycle arrest. The large guard cells also displayed nuclei with relative sizes of around 4.0 but contained 20 chromosomes, which corresponds to a tetraploid chromosome number (4*n*). This indicates that endomitosis, but not endoreplication, had occurred in the developmental processes of the large guard cells and that endomitosis had occurred only once in such processes. The nuclei of *gigas* cells also contained 20 chromosomes, but their sizes were discretely distributed from 8 to 32 (Figure 2D). One explanation is that endomitosis had occurred just one time prior to one to three rounds of endoreplication during the production of *gigas* cells.

The occurrence of endomitosis was confirmed by live-cell imaging of cotyledon epidermis in which microtubule arrays and chromosomes were labeled by GFP-TUA6 and H2B-tdTomato, respectively. We observed epidermal cells undergoing normal progression of mitosis and cytokinesis in wild-type cotyledons

(Figure 3A; see Supplemental Movie 1 online). In *gig1-1 myb3r4* cotyledons, however, we occasionally observed that condensed chromosomes failed to transition into anaphase in a timely fashion and remained in a condensed state for 1.5 to 2.0 h before separation of sister chromatids took place (Figure 3B; see Supplemental Movie 2 online), which only takes 10 to 15 min in the wild type (Figure 3A; see Supplemental Movie 1 online). After separation, sister chromatids could not further move toward spindle poles; instead, they merged into a single entity, resulting in the generation of a single polyploid nucleus. Moreover, in those cells, phragmoplasts were not properly formed between separated sister chromatids; instead, microtubules accumulated in the cytoplasm at one edge of the cell, resulting in the failure of the entire process of cytokinesis (Figure 3B; see Supplemental Movie 2 online).

Endomitosis Occurs Early in Stomatal Development in *gig1* Mutants

To discern the developmental processes of the large guard cells and the *gigas* cells, we analyzed cell division history using TMM:GUS-GFP, which marks dividing and recently divided stomatal precursor cells (Figures 4A and 4B). The large guard cells containing 20 chromosomes are typically surrounded by a group of small cells expressing TMM:GUS-GFP, and these cells contained 20 chromosomes, which are further surrounded by cells with 10 chromosomes. This suggests that the occurrence of endomitosis in stomatal lineage cells might have produced a tetraploid cell that then divided several times to produce the tetraploid guard cells. By contrast, cells surrounding a *gigas* cell carried 10 chromosomes and did not express TMM:GUS-GFP, suggesting that a tetraploid cell that had been produced by endomitosis underwent endoreplication, but not cell division, to generate the *gigas* cells. Next, we showed that cells expressing SPCH-GFP and EPF2:GFP, which mark precursor cells characteristic of the initial stage of stomatal development (i.e., meristemoid mother cells and the meristemoid) (Pillitteri et al., 2007; Hara et al., 2009), had already enlarged or contained enlarged nuclei (Figures 4C to 4F). Therefore, it can be speculated that endomitosis had occurred in the early stages of stomatal development and that the resulting tetraploid cells later produced either the large guard cells or the *gigas* cells. The *gigas* cells, possessing characteristics of both guard cells and pavement cells, might have originated by the occurrence of endomitosis in place of asymmetric division, which would normally segregate stomatal and pavement cell fates (Ten Hove and Heidstra, 2008), and such failed asymmetric division might produce cells with a mixed fate.

Molecular Identification of *GIG1*

We identified *GIG1* via the map-based cloning and sequencing of the mutant genome. We found base substitutions in At3g57860 in both *gig1-1* and *gig1-2* (Figure 5A). The *gig1-1* mutation changes Val at position 42 into Met, while, in *gig1-2*, the G-to-A substitution at the 3′ splice site of intron 2 results in splicing variants encoding truncated GIG1 (see Supplemental Figure 6 online). This suggests that *gig1-2* is a null allele of *GIG1*, which is consistent with the stronger phenotype in *gig1-2* in comparison with *gig1-1*. An additional mutant allele, *gig1-3*, was identified in the collection of RIKEN transposon insertion lines (Kuromori et al., 2004), and homozygous *gig1-3* mutation resulted in a similar phenotype in cotyledons. Furthermore, introduction of a genomic fragment of At3g57860 into *gig1-2* homozygotes completely abolished the *gig1* phenotype in cotyledons, confirming that *GIG1* was At3g57860 (see Supplemental Figure 7 online).

Double Mutation of *GIG1* and *UVI4* Is Lethal

At3g57860 was previously identified as *OMISSION OF SECOND DIVISION1* (*OSD1*) in a reverse genetic approach, and its

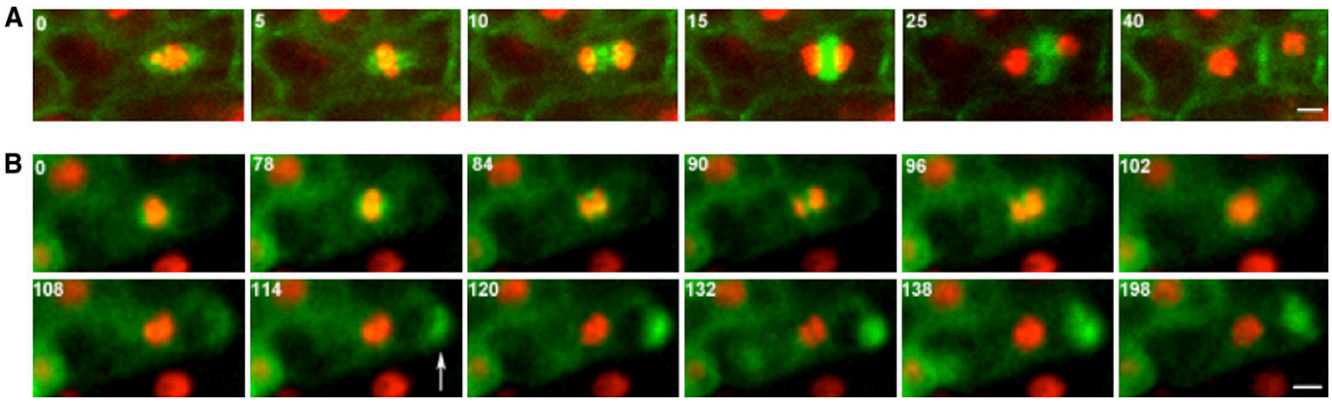

Figure 3. Live-Cell Imaging of the Epidermal Cells of Cotyledons.

(A) Asymmetric cell division of the meristemoid mother cell in wild-type cotyledons.
(B) Endomitosis occurred in the meristemoid mother cell in the *gig1-1 myb3r4* cotyledons.
Signals of GFP-TUA6 for tubulins and H2B-tdTomato for chromosomes are shown in green and red, respectively. The overlapping signals represent yellow. The number on the top left indicates elapsed time from the start of imaging in minutes. An arrow indicates microtubules accumulated in the cytoplasm at one edge of the cell. Bars = 5 μm.

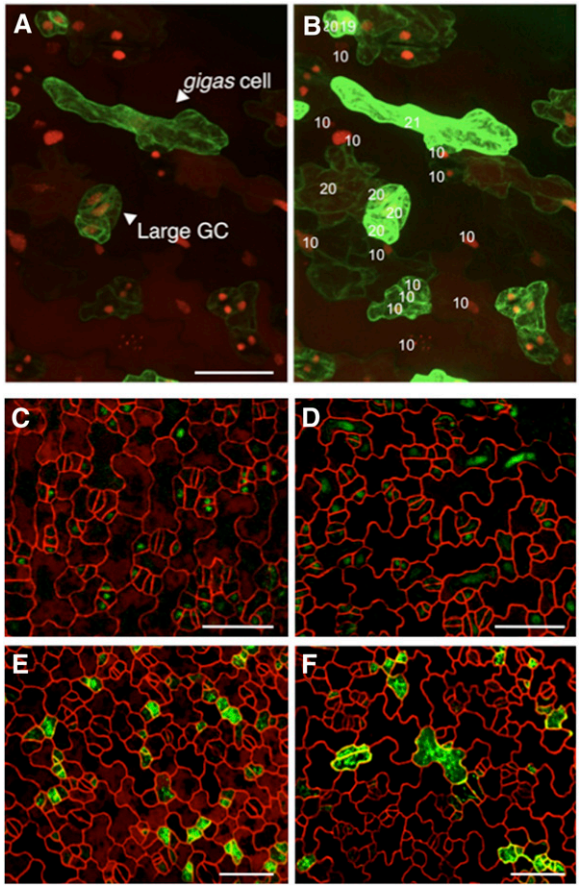

Figure 4. The Occurrence of Endomitosis in Developing *gig1-1 myb3r4* Cotyledons.

(A) and **(B)** Cell lineage analysis of *gigas* cells and large guard cells in *gig1-1 myb3r4* cotyledons. Cell division history can be estimated by expression of TMM:GUS-GFP and cell patterns. The image shown in **(A)** is enhanced in **(B)** to show weak GFP signals in cells surrounding large guard cells. Chromosome numbers in each nucleus, as determined by tdTomato-CENH3 signals (shown in red), are indicated **(B)**. TMM:GUS-GFP signals are in green and tdTomato-CENH3 signals in red.

(C) and **(D)** SPCH-GFP signals in developing cotyledons of the wild type **(C)** and *gig1-1 myb3r4* mutant **(D)**.

(E) and **(F)** EPF2:GFP signals in developing cotyledons of the wild type **(E)** and *gig1-1 myb3r4* mutant **(F)**.

Cell outlines were counterstained with FM4-64 (shown in red) in **(C)** to **(F)**. Bars = 50 μm.

homozygous mutation generates diploid pollen due to the absence of meiosis II in male gametophyte development (d'Erfurth et al., 2009). The diploid pollen was also observed in homozygotes of the strong *gig1-2* allele but not of the weak *gig1-1* allele (see Supplemental Figure 8 online). The *Arabidopsis* genome encodes a gene (At2g42260) that is paralogous to *GIG1* (d'Erfurth et al., 2009), which was previously identified as *POLYCHOME*/*UVI4* in two independent forward genetic screens (Figure 5A) (Perazza et al., 1999; Hase et al., 2006). It has been reported that a homozygous recessive *pym*/*uvi4* mutation causes overbranched trichomes that were associated with the promotion of endoreplication (Perazza et al., 1999; Hase et al., 2006). To test the functional redundancy between *GIG1* and *UVI4*, we made crosses between null alleles of *GIG1* (*gig1-2*) and *UVI4*. We could not obtain double *gig1-2 uvi4* mutants in the F2 generation, suggesting that the double mutation was lethal. Reciprocal cross experiments suggested that transmission of double mutant gametes was significantly reduced by ~45% on the female side (P value = 0.018, χ^2 test), whereas it was normally transmitted on the male side (P value = 0.53, χ^2 test). Consistent with these results, we observed a reduced number of enlarged nuclei in the female, but not male, gametophyte in *gig1-2*/+ *uvi4*/*uvi4* plants (Figures 5B to 5D). We also found developing seeds with a reduced number of abnormally enlarged nuclei in the endosperm (Figures 5E and 5F). Mitotic figures of nuclei in such malformed endosperms contained an increased number of chromosomes (Figures 5G and 5H), suggesting the occurrence of endomitosis. Our results showed that functions of *GIG1* and *UVI4* may at least be partially redundant and support essential roles of these genes in nuclear division during gametogenesis and endosperm development.

Expression of *GIG1*

Expression of *GIG1* was analyzed in plants transformed with the upstream region of *GIG1* (1.6 kb) fused to the reporter gene, GUS, or nuclear-localized yellow fluorescent protein (YFP). GUS expression was observed in the shoot apical meristem and young leaves, which are rich in rapidly dividing cells (Figures 5I and 5J). In the epidermis of cotyledons and leaves, expression of YFP was observed in dividing and recently divided stomatal precursor cells, especially in dividing guard mother cells and young guard cells (Figure 5K). Consistent with the mixed-fate nature of *gigas* cells, we also observed YFP expression in asymmetrically dividing meristemoid mother cells and meristemoids (Figure 5L). In roots, YFP was expressed preferentially in the division zones of root tips (Figures 5M). These data suggest that *GIG1* expression is associated with cell division but also with specific cell types.

GIG1 and UVI4 Physically Interact with APC/C Activators

It was recently shown by proteomic studies that GIG1 and UVI4 associate in vivo with the APC/C in cultured *Arabidopsis* cells (Van Leene et al., 2010). The functional relevance of this physical interaction between GIG1/UVI4 and APC/C remained unknown. Interestingly, we observed that *GIG1* overexpression leads to a similar dwarf phenotype that is caused by knockdown of the APC/C core subunit genes (Figures 6A and 6B) (Saze and Kakutani, 2007; Marrocco et al., 2009). This suggests that *GIG1* might inhibit the activity of APC/C through protein–protein interaction. We examined which components of APC/C physically bind with GIG1 and UVI4 by yeast two-hybrid assays (Figure 6C) and showed that both GIG1 and UVI4 interacted with all APC/C activators tested (CCS52A1/FZR2, CCS52B/FZR3, CDC20.1, and CDC20.5), whereas no obvious interaction was observed for core subunits of APC/C (APC2, APC7, APC10, CDC27a, and HBT). This suggests that GIG1 and UVI4 may inhibit APC/C

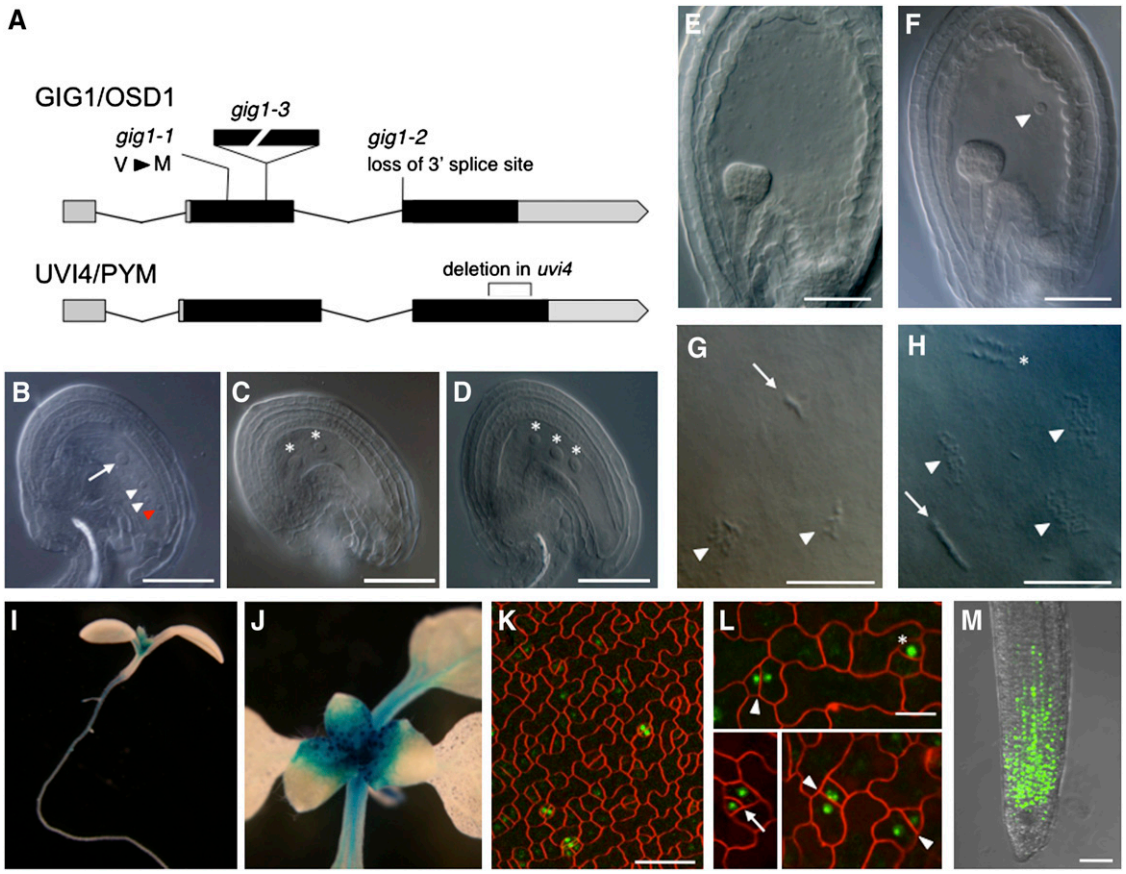

Figure 5. Essential Redundant Functions of *GIG1* and *UVI4*.

(A) Schematic representation of *GIG1* and *UVI4* and their mutant alleles. Exons and introns are shown by boxes and lines, respectively, where black and gray boxes indicate coding and noncoding regions, respectively.

(B) to **(D)** GIG1 and UVI4 may have essential roles in megagametophyte development. The mature wild-type megagametophyte contains one large polar nucleus (white arrow) and small nuclei in two synergids (white arrowheads) and one egg cell (red arrowhead) **(B)**. By contrast, malformed megagametophytes found in *gig1-2*/+ *uvi4*/*uvi4* ovaries contained a reduced number of enlarged nuclei (shown by asterisks) **([C]** and **[D])**.

(E) and **(F)** GIG1 and UVI4 may have essential roles in endosperm development. Developing wild-type endosperm **(E)** and developing endosperm with enlarged and reduced numbers of nuclei found in *gig1-2*/+ *uvi4*/*uvi4* ovaries **(F)**. One enlarged nucleus in focus is indicated by an arrowhead.

(G) and **(H)** Loss of *GIG1* and *UVI4* generates polyploid endosperm nuclei. Mitotic figures of endosperm nuclei were observed by DIC in normal **(G)** and abnormal **(H)** ovules that were segregated in *gig1-2*/+ *uvi4*/*uvi4* ovaries. Arrowheads indicate chromosomes at prophase or prometaphase. Arrows and asterisks indicate chromosomes at metaphase and anaphase, respectively.

(I) and **(J)** Expression of the GUS reporter gene driven by the *GIG1* promoter in wild-type seedlings at 7 **(I)** and 11 **(J)** d after germination.

(K) to **(M)** Expression of nuclear-localized YFP driven by the *GIG1* promoter in wild-type seedlings. Shown are cotyledons at 3 **(K)** and 5 d **(L)** and a root at 7 d **(M)** after germination. YFP signals are shown in green. Cell outlines were visualized by counterstaining with FM4-64 (shown in red) **([K]** and **[L])**. YFP signals of root tip in 7-d-old seedlings are merged with DIC image **(M)**. Dividing or recently divided stomatal precursor cells are indicated by symbols in **(L)** as follows: arrowhead, meristemoid mother cell; arrow, meristemoid; and asterisk, guard mother cell.

Bars = 50 μm in **(B)** to **(F)**, **(K)**, and **(M)** and 20 μm in **(G)**, **(H)**, and **(L)**.

through preventing the APC/C activation mediated by FZR/CDH1 and FZY/CDC20.

Genetic Interaction of *GIG1* and *UVI4* with APC/C

We further analyzed the genetic interactions between *GIG1* and the APC/C using the *35S:APC10* cosuppression line with decreased expression of *APC10*, a gene encoding a core subunit of APC/C (Marrocco et al., 2009). Our genetic analysis showed that the *gigas* cell phenotype was suppressed in *gig1-2*/*gig1-2* cotyledons that retained the *35S:APC10* transgene, while such suppression was not observed in the segregants that had lost the *35S:APC10* transgene (Figure 6D). Our interpretation is that the *gig1-2* mutant may have increased APC/C activity, causing endomitosis; however, when elevated APC/C activity is downregulated by decreased expression of *APC10*, endomitosis is suppressed.

We also tested for genetic interactions between the *gig1* mutation and APC/C activators. Among the four APC/C activators tested in yeast two-hybrid assays, we selected CDC20.1

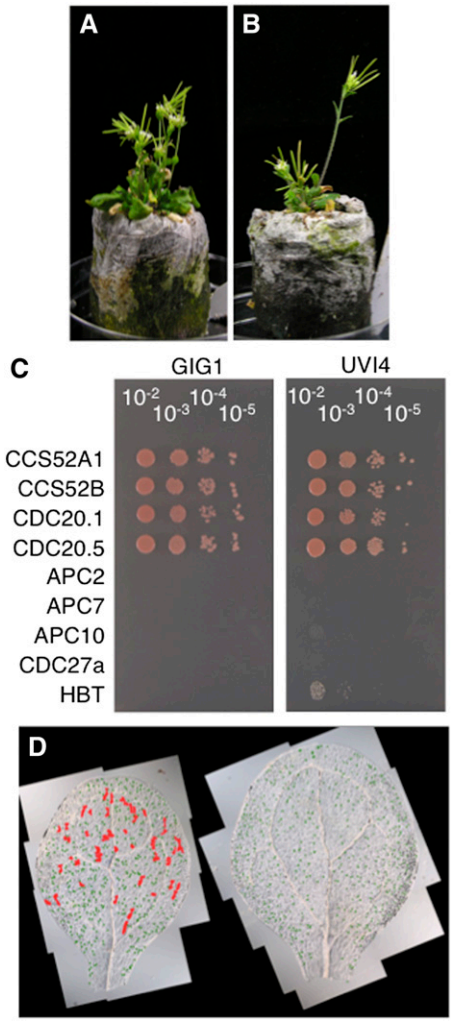

Figure 6. GIG1 and UVI4 May Inhibit APC/C Activity.

(A) and **(B)** Dwarf phenotypes of *GIG1*-overexpressing **(A)** and *APC10*-knockdown **(B)** plants. Shown are plants from the CDKA;1:GIG1 transgenic line **(A)** and 35S:APC10 cosuppression line **(B)** that were grown for 40 d.

(C) GIG1 or UVI4 interact with APC/C activators in yeast cells. A yeast two-hybrid assay was performed to test the interactions of GIG1 and UVI4 with APC/C activators (CCS52A1/FZR2, CCS52B/FZR3, CDC20.1, and CDC20.5) and core subunits (APC2, APC7, APC10, CDC27a, and HBT). Numbers on each image indicate dilution rate of yeast cell suspension.

(D) Suppression of the *gigas* cell phenotype by decreased expression of *APC10*. Cotyledons from *gig1-2* homozygotes with (right) or without (left) cosuppression of *APC10* were viewed with DIC. Guard cells and *gigas* cells are shown in green and red, respectively.

and CCS52B/FZR3 for our genetic analysis because these two genes are known to be preferentially expressed in dividing cells, in which *GIG1* is also strongly expressed (Larson-Rabin et al., 2009; Kevei et al., 2011). To obtain a high expression of these genes in dividing cells, we used the *CDKA;1* promoter, whose activity is associated with dividing *Arabidopsis* cells (Hemerly et al., 1993). When an overexpression construct, *CDKA;1*:*CDC20.1*, was introduced into *gig1-1 myb3r4* plants, the *gig1* phenotype was markedly enhanced, increasing the frequency of *gigas* cells and, more dramatically, that of the round cells (Figures 7A and 7B), whereas the introduction of *CDKA;1*:*CCS52B* showed no such effects (Figure 7C). Even greater enhancing effects were observed when *CDC20.1* was overexpressed under the promoter of *EPF2* (Figure 7D). Conversely, *CDKA;1*:*CCS52B* caused a dramatic enhancement of endoreplication in *uvi4* root tips, whereas no such effect was observed in the case of *CDKA;1*:*CDC20.1* (Figures 7E to 7G; see Supplemental Figure 9 online). Similar differential effects were observed for trichome overbranching and dwarf phenotypes in *uvi4* (see Supplemental Figure 10 online). We did not observe such prominent effects when *CDC20.1* and *CCS52B*/*FZR3* were overexpressed in the wild type (see Supplemental Figure 11 online). All our data are generally consistent with the idea that GIG1 and UVI4 may act as inhibitors of the APC/C. It is also noted that there may be some functional differences between GIG1 and UVI4 because their loss-of-function causes different phenotypes, which are affected differently by the overexpression of CCS52B/FZR3 and CDC20.1.

Modified *GIG1* Function Affects the Levels of Mitotic Cyclins

To test if decreased expression of mitotic cyclins, well-known substrates of APC/C, is critical for the endomitosis phenotype in *gig1* cotyledons, we examined the effects of *cycb2;2* mutations in the *gig1* mutant background (Figures 7H and 7I). We found that the additional *cycb2;2* mutation significantly enhanced endomitosis phenotype in *gig1-1* plants.

To examine the actual effects on cyclin expression, we made a CYCB1;2-YFP construct in which YFP fused to the N-terminal region of CYCB1;2, which contained the destruction box motif, was placed under its own promoter (proCYCB1;2:dBox-YFP). We observed that expression of CYCB1;2-YFP was dramatically increased by *GIG1* overexpression under the dexamethasone-inducible promoter, causing strong and uniform YFP expression in root tips (Figure 7J, right), which otherwise shows patchy expression pattern (Figure 7J, left). Overexpression of *UVI4* caused similar but less prominent effects (see Supplemental Figure 12 online). Our quantitative RT-PCR analysis indicated that overexpression of neither GIG1 nor UVI4 affects significantly the transcription of mitotic cyclins, supporting our idea that these proteins affect mitotic cyclin stability (see Supplemental Figure 12 on line).

DISCUSSION

GIG1 Is a Novel Plant-Specific Inhibitor of APC/C

Activity of APC/C is generally regulated by both activator and inhibitor proteins. The APC/C activators CDC20/FZY and CDH1/FZR activate APC/C at different points in the cell cycle and also bind to the target proteins of APC/C for selective substrate recognition (Pesin and Orr-Weaver, 2008). CDC20/FZY and CDH1/FZR are related to each other and conserved in all

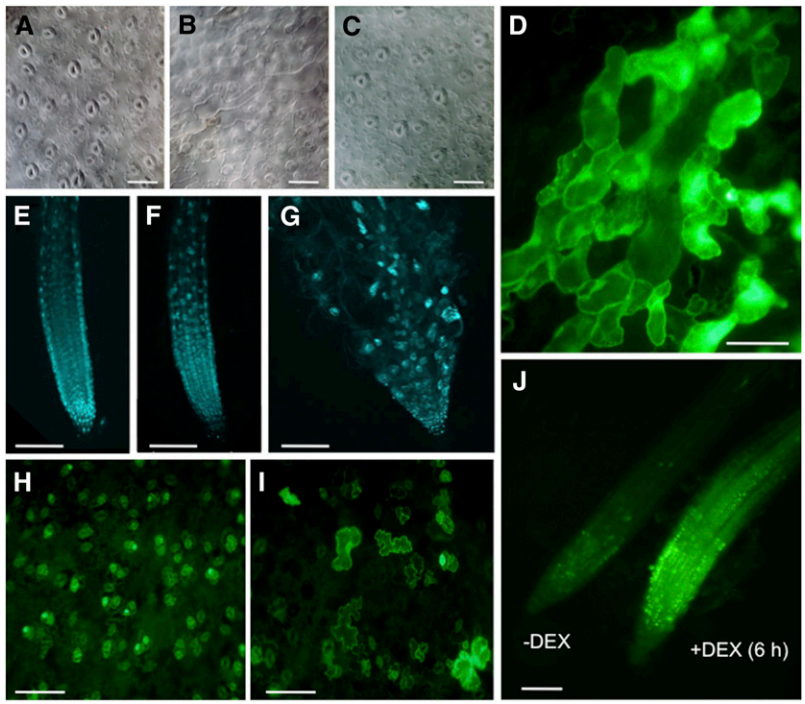

Figure 7. GIG1 and UVI4 May Inhibit APC/C Activation and Stabilize Mitotic Cyclins.

(A) to **(C)** Effects of overexpression of *CCS52B/FZR3* and *CDC20.1* in leaves of *gig1-1 myb3r4* seedlings. DIC images of *gig1-1 myb3r4* seedlings **(A)** and of *gig1-1 myb3r4* seedlings transformed with CDKA;1:CDC20.1 **(B)** and CDKA;1:CCS52B **(C)**.

(D) Enhanced *gigas* cell phenotype in leaves of *gig1-1 myb3r4* seedlings transformed with EPF2:CDC20.1. TMM:GUS-GFP signals are shown in green.

(E) to **(G)** Effects of overexpression of *CCS52B/FZR3* and *CDC20.1* on the roots of *uvi4* seedlings. Roots of *uvi4* seedlings **(E)** and of those transformed with CDKA;1:CDC20.1 **(F)** and CDKA;1:CCS52B **(G)** were stained with DAPI.

(H) and **(I)** The *cycb2;2* mutation enhanced the *gigas* cell phenotype in *gig1-1* seedlings. Developing cotyledons from *gig1-1* single mutants **(H)** and double *gig1-1 cycb2;2* mutants **(I)**. TMM:GUS-GFP signals are shown in green.

(J) Overexpression of *GIG1* causes accumulation of CYCB1;2-YFP. Seedlings transformed with the proCYCB1;2:dBox-YFP construct are cultured with 10 μM dexamethasone (DEX) for induction of *GIG1* overexpression (right) or without dexamethasone as a control (left). YFP signals are shown in green.

Bars = 40 μm in **(A)** to **(D)** and 100 μm in **(E)** to **(J)**.

eukaryotic species. In vertebrates, the negative regulation of APC/C is typically achieved by two related proteins, Emi1 and Emi2, which bind to APC/C activators and the core complex (Barford, 2011). The primary function of Emi1 is to inhibit APC/C^{FZR} and thereby terminate DNA replication in a timely fashion and enable the transition from the G2 to M phases (Grosskortenhaus and Sprenger, 2002; Machida and Dutta, 2007), while Emi2 inhibits APC/C^{CDC20} and thereby enables the proper progression through meiosis (Madgwick et al., 2006). Plants do not have counterparts of vertebrate Emi1 and Emi2, and it remains unclear if plants also have a negative regulator of APC/C. Our results suggest that GIG1 and UVI4 may correspond to such negative regulators of APC/C. This is supported by the fact that these proteins both interact with APC/C activators. Moreover, *GIG1* overexpression phenocopies the downregulation of APC/C. Our genetic interaction studies also support a model in which GIG1 and UVI4 negatively regulate APC/C activity. For instance, the *gig1-2* mutant phenotype that may result from increased APC/C activity can indeed be suppressed by decreasing APC/C activity. Finally, the overaccumulation of CYCB1;2-YFP in *GIG1*-overexpressing plants also fits this model. We showed that GIG1 and UVI4 may have partially overlapping functions that are essential for female gametogenesis and endosperm development. In these developmental processes, *GIG1* and *UVI4* may be required for the accumulation of still unknown mitotic regulators by inhibiting their degradation.

Difference in GIG1 and UVI4 Functions

Besides having overlapping functions, GIG1 and UVI4 also have specific roles in mitotic regulation. We showed that mutations in *GIG1* and *UVI4* preferentially affect the increase in cellular ploidy caused by endomitosis and endoreplication, respectively. Whereas endoreplication results from arresting cells at the G2 phase before they enter mitosis, endomitosis results from arresting cells within the M phase before they complete mitosis (Edgar and Orr-Weaver, 2001). This suggests that UVI4 may function earlier than GIG1 in mitotic cell cycle. Probably, UVI4 may act at the G2-to-M transition by promoting the accumulation of specific mitotic cyclins, such as CYCA2;3, which has been identified as a negative regulator of endoreplication (Imai et al., 2006). Loss of *UVI4* may thus result in a reduced amount of such cyclins, thereby accelerating the onset of endoreplication. On the

other hand, GIG1 may act later during mitosis for the scheduled degradation of mitotic regulators, such as CYCB2;2, whose amount was critical for ectopic occurrence of endomitosis in *gig1*. In this respect, it has been shown that tobacco (*Nicotiana tabacum*) cells expressing nondestructible cyclin B1 exhibit doubled DNA content as a result of endomitosis (Weingartner et al., 2004).

Our data also suggested that GIG1 and UVI4 may preferentially affect the activities of APC/C^{CDC20} and APC/C^{FZR}, respectively. Overexpression of CDC20.1 caused a severe endomitosis phenotype in *gig1* but not in *uvi4*, while overexpression of CCS52B/FZR3 resulted in enhanced endoreplication in *uvi4* but less efficient enhancement in *gig1*. It is generally known that CDC20-type APC/C activators execute their function specifically during mitosis, while FZR-type activators can function during interphase (Pesin and Orr-Weaver, 2008). This is consistent with our idea that GIG1 and UVI4 have temporally different activities in the cell cycle. GIG1 may prevent the ectopic occurrence of endomitosis by selective inhibition of APC/C^{CDC20} during mitosis, while UVI4 may negatively regulate endoreplication onset by inhibiting APC/C^{FZR} at the G2 to M transition.

A Role for APC/C in Cell Fate Determination?

The most striking phenotype of *gig1* is the generation of *gigas* cells, which display characteristics of both guard cells and pavement cells. During epidermal development in *Arabidopsis*, meristemoid mother cells divide asymmetrically to generate two daughter cells that follow either one of the two developmental pathways, ultimately generating guard cells or pavement cells (Nadeau, 2009). Our examination of *gigas* cells showed that they have guard cell–like identities and share a developmental pathway with stomatal lineage cells. At the same time, these cells are similar to pavement cells in terms of size and morphology. The occurrence of endoreplication in developing *gigas* cells, which is absent in the developmental pathway that generates guard cells, may also be explained by pavement cell–like characteristics in the mixed-fate cells. The occurrence of endomitosis in place of asymmetric division of either meristemoid mother cells or meristemoids may produce single cells with identities of both daughter cells during the generation of *gigas* cells.

However, failure of cell division alone may not account for the generation of mixed-fate cells in the epidermis. Many mutations are known in *Arabidopsis* that cause incomplete cytokinesis in epidermal cells; none of them, however, was reported to produce cells with such a mixed fate (Jürgens, 2005). Similarly, it is well known that the application of antimicrotubule drugs, such as colchicines, causes transient arrest at mitosis and generates polyploid somatic cells (Eigsti, 1938; Levan, 1938). Even though colchicine has long been used to produce polyploid plants, the occurrence of such mixed-fate cells has not been reported upon application of the drug. These observations led us to hypothesize that APC/C may be involved in the determination of epidermal cell fate in addition to its role in mitotic progression. The unexpected roles of APC/C in the determination of cell identity may not be specific for stomatal development, since recent findings have suggested similar nonmitotic roles of APC/C in some different contexts, which include differentiation of the lens and axons in animals (Wu et al., 2007; Yang et al., 2009), as well as vascular development and maintenance of stem cell identity in plants (Marrocco et al., 2009; Vanstraelen et al., 2009).

In summary, we identified novel APC/C inhibitors in *Arabidopsis*, which may have a role in cell fate determination. Future genetic and biochemical studies will uncover the mechanisms that link the cell cycle to asymmetric cell fate determination, as well as the upstream and downstream signaling pathways of these inhibitors.

METHODS

Plant Materials

Arabidopsis thaliana Columbia (Col) was used as the wild type. All mutants and transgenic lines are in the Col background, except for *gig1-3* and KAT1:GUS, which are in the Nossen and RLD1 background, respectively. The *gig1* mutant lines, *gig1-1* and *gig1-2*, were derived from an ethyl methanesulfonate–mutagenized *myb3r4-1* population and backcrossed four times before analysis. Another allele of *GIG1* (*gig1-3*, pst15307), which has a *Ds* transposon insertion in exon 2, was obtained from the Plant Functional Genomics Research Group of RIKEN Genomic Sciences Center (Kuromori et al., 2004). Other mutants and transgenic plants, enhancer trap lines E994 and E1728, TMM:GUS-GFP, KAT1:GUS, SPCH-GFP, EPF2:GFP, GFP-TUA6, H2B-tdTomato, and *spch-3* were described previously (R.L. Nakamura et al., 1995; Nadeau and Sack, 2002; M. Nakamura et al., 2004; Ohashi-Ito and Bergmann, 2006; Pillitteri et al., 2007; Hara et al., 2009; Adachi et al., 2011).

Map-Based Cloning of GIG1

The genetic screen was conducted by mutagenizing ~20,000 *myb3r4-1* seeds with 0.3% ethyl methanesulfonate (Sigma-Aldrich) for 10 h. The cotyledon was removed from each M2 plant, mounted after clearing, and visually screened for abnormality in stomatal shape with DIC microscopy. From a screen of 5000 M2 seedlings, two alleles of *GIG1* were identified. A mapping population was generated by outcrossing to Landsberg *erecta* (L*er*). DNA markers were used to detect polymorphisms between Col and L*er*. The markers were designed based on the information available in the Monsanto Arabidopsis Polymorphism and L*er* Sequence Collection (http://www.Arabidopsis.org/browse/Cereon/index.jsp).

Microscopy

Microscopy observations with DIC and fluorescent optics were done as described previously (Haga et al., 2007). For images of epidermal cell patterns, live tissues were mounted in water and visualized using an Olympus FV1000 confocal microscope. For counterstaining of cell outlines, tissues were placed in 10 μM solution of FM4-64 (Molecular Probes) for 2 min. GFP was excited at 473 nm, and fluorescence was detected at 485 to 545 nm, FM4-64 was excited at 559 nm, and fluorescence was detected at 570 to 670 nm.

Clearing of plant materials, histochemical GUS assay, and 4′,6-diamidino-2-phenylindole (DAPI) staining were performed as described previously (Haga et al., 2007, 2011). Scanning electron microscopy was performed as described previously (Semiarti et al., 2001).

Imaging Analysis

To determine kinetochore number, fluorescent signals of tdTomato-CENH3 in epidermis were counted using Metamorph version 7.5 (Molecular Devices). Imaging was performed using a fluorescence microscope (IX-81; Olympus) equipped with a confocal laser scanner unit

CSUX-1 (Yokogawa Electronic) and a charge-coupled device camera (CoolSNAP HQ2; Roper Scientific) as described previously (Adachi et al., 2011). Live-cell imaging of the cotyledon epidermis in 2- to 3-d-old seedlings with H2B-tdTomato and GFP-TUA6 was performed as described previously (Kosetsu et al., 2010).

Plasmid Construction and Transformation

See Supplemental Table 1 online for a list of plasmid constructs generated in this study and Supplemental Table 2 online for a list of primer DNA sequences used for generating these plasmids. Generation and selection of transgenic plants were done as described previously (Haga et al., 2007). Binary vectors, pPZP211, pTA7001, pBGGUS, and pBGYN, were previously described (Hajdukiewicz et al., 1994; Aoyama and Chua, 1997; Kubo et al., 2005)

Yeast Two-Hybrid Assays

Yeast two-hybrid assays were performed as described by Soyano et al. (2003). *Saccharomyces cerevisiae* strain L40 was cotransformed with pBTM116- and pVP16-based plasmids carrying different cDNAs. A single colony was diluted with water and spotted on medium lacking His that was supplemented with 5 mM 3-amino-1,2,4-triazole and cultured at 30°C for 2 d.

Quantitative Real-Time PCR

Extraction of total RNA and synthesis of first-strand cDNA were performed as described previously (Haga et al., 2007). Quantitative real-time PCR was performed using the SYBR PremixEx Taq (Perfect Real Time) kit (TaKaRa Biomedical) on the LightCycler480 machine (Roche Diagnostics). See Supplemental Table 3 online for a list of primer DNA sequences used for real-time PCR.

Accession Numbers

Arabidopsis Genome Initiative numbers for the genes discussed in this article are as follows: *APC2*, AT2G04660; *APC7*, At2g39090; *APC10*, At2g18290; *CDC20.1*, At4g33270; *CDC20.5*, At5g27570; *CDC27a*, AT3G16320; *CYCA2;3*, At1g15570; *CYCB1;2*, At5g06150; *CYCB2;2*, At4g35620; *EPF2*, At1g34245; *CCS52A1/FZR2*, At4g22910; *CCS52B/FZR3*, At5g13840; *GIG1/OSD1*, At3g57860; *HBT*, At2g20000; *UVI4*, At2g42260; *KAT1*, At5g46240; *SPCH*, At5g53210; and *TMM*, At1g80080.

Supplemental Data

The following materials are available in the online version of this article.

Supplemental Figure 1. Schematic Representation of Endoreplication and Endomitosis.

Supplemental Figure 2. Abnormalities of Epidermal Cells in *gig1* Cotyledon Are Enhanced by *myb3r4* and Double *myb3r1 myb3r4* Mutations.

Supplemental Figure 3. Expression of Guard Cell–Specific Markers in *gig1* Cotyledons.

Supplemental Figure 4. *Gigas* Cells Contain Enlarged Nuclei with Abnormal Shapes.

Supplemental Figure 5. Abnormal Guard Cells in *gig1* Epidermis.

Supplemental Figure 6. Splice Variants Generated from the *gig1-2* Allele.

Supplemental Figure 7. Complementation of *gigas* Cell Phenotype in *gig1* Epidermis.

Supplemental Figure 8. *gig1-2* but Not *gig1-1* Plants Produce Enlarged Pollen Grains with Increased Sizes of Nuclei.

Supplemental Figure 9. Overexpression of *CCS52B/FZR3* Severely Affects Cell Patterns in *uvi4* Roots.

Supplemental Figure 10. Phenotypes of *uvi4* Are Enhanced by Overexpression of *CCS52B/FZR3*.

Supplemental Figure 11. DAPI-Stained Root Tips in CDC20.1- and CCS52B/FZR3-Overexpressing Plants in the Wild-Type Background.

Supplemental Figure 12. Overexpression of *GIG1* and *UVI4* Causes Stabilization of CYCB1;2-YFP.

Supplemental Table 1. List of Plasmid Constructs Used in This Study and Their Description.

Supplemental Table 2. List of Primers and Their DNA Sequences Used for Plasmid Construction.

Supplemental Table 3. List of Primers and Their DNA Sequences Used for Real-Time PCR.

Supplemental Movie 1. Live-Cell Imaging of a Wild-Type Epidermal Cell Expressing GFP-TUA6 and H2B-tdTomato.

Supplemental Movie 2. Live-Cell Imaging of a *gig1 myb3r4* Epidermal Cell Expressing GFP-TUA6 and H2B-tdTomato.

Supplemental Movie Legends. Legends for Supplemental Movies 1 and 2.

ACKNOWLEDGMENTS

We thank Kanako Komatsu, Chie Kotani, and Yuka Sako for technical assistance and Yasunori Machida and Masahiro Kanaoka for helpful discussion. We thank Keiko Torii for GFP marker lines (E994 and SPCH-GFP) and the *spch* mutant, Fred Sack for TMM:GUS-GFP, Yoshihiro Hase for the *uvi4* mutant, Tatsuo Kakimoto for EPF2:GFP, Taku Demura for the pBGYN vector, Takashi Hashimoto for GFP-TUA6, and Michiko Sasabe and Yasunori Machida for pVP16S and pBTM116E1 plasmids. This work was supported by Grants-in-Aid from the Japan Society for the Promotion of Science (Grants 22570040 and 0008) and from the Ministry of Education, Culture, Sports, Science and Technology (Grants 23119508 and 23012017) and by the Yamada Science Foundation.

AUTHOR CONTRIBUTIONS

M.I., P.G., M.-C.C., and S.M. designed the research. M.I., S.M., E.I., S.I., M.K., M.-C.C., and Y.Y. performed the research. M.I., S.M., E.I., S.I., and Y.Y. analyzed the data. M.I., S.M., and P.G. wrote the article.

Received September 23, 2011; revised November 3, 2011; accepted November 20, 2011; published December 13, 2011.

REFERENCES

Adachi, S., et al. (2011). Programmed induction of endoreduplication by DNA double-strand breaks in Arabidopsis. Proc. Natl. Acad. Sci. USA **108:** 10004–10009.

Aoyama, T., and Chua, N.H. (1997). A glucocorticoid-mediated transcriptional induction system in transgenic plants. Plant J. **11:** 605–612.

Barford, D. (2011). Structure, function and mechanism of the anaphase promoting complex (APC/C). Q. Rev. Biophys. **44:** 153–190.

Beemster, G.T., De Veylder, L., Vercruysse, S., West, G., Rombaut, D., Van Hummelen, P., Galichet, A., Gruissem, W., Inzé, D., and Vuylsteke, M. (2005). Genome-wide analysis of gene expression profiles associated with cell cycle transitions in growing organs of Arabidopsis. Plant Physiol. **138:** 734–743.

Boudolf, V., Barrôco, R., Engler, Jde.A., Verkest, A., Beeckman, T., Naudts, M., Inzé, D., and De Veylder, L. (2004). B1-type cyclin-dependent kinases are essential for the formation of stomatal complexes in *Arabidopsis thaliana*. Plant Cell **16:** 945–955.

Breuer, C., Ishida, T., and Sugimoto, K. (2010). Developmental control of endocycles and cell growth in plants. Curr. Opin. Plant Biol. **13:** 654–660.

Cebolla, A., Vinardell, J.M., Kiss, E., Oláh, B., Roudier, F., Kondorosi, A., and Kondorosi, E. (1999). The mitotic inhibitor ccs52 is required for endoreduplication and ploidy-dependent cell enlargement in plants. EMBO J. **18:** 4476–4484.

D'Amato, F. (1984). Role of polyploidy in reproductive organs and tissues. In Embryology of the Angiosperms, B.M. Johri, ed (Berlin: Springer-Verlag), pp. 519–566.

d'Erfurth, I., Jolivet, S., Froger, N., Catrice, O., Novatchkova, M., and Mercier, R. (2009). Turning meiosis into mitosis. PLoS Biol. **7:** e1000124.

De Veylder, L., Larkin, J.C., and Schnittger, A. (2011). Molecular control and function of endoreplication in development and physiology. Trends Plant Sci. **16:** 624–634.

Edgar, B.A., and Orr-Weaver, T.L. (2001). Endoreplication cell cycles: More for less. Cell **105:** 297–306.

Eigsti, O.J. (1938). A cytological study of colchicine effects in the induction of polyploidy in plants. Proc. Natl. Acad. Sci. USA **24:** 56–63.

Eloy, N.B., de Freitas Lima, M., Van Damme, D., Vanhaeren, H., Gonzalez, N., De Milde, L., Hemerly, A.S., Beemster, G.T., Inzé, D., and Ferreira, P.C. (2011). The APC/C subunit 10 plays an essential role in cell proliferation during leaf development. Plant J. **68:** 351–363.

Falbel, T.G., Koch, L.M., Nadeau, J.A., Segui-Simarro, J.M., Sack, F.D., and Bednarek, S.Y. (2003). SCD1 is required for cytokinesis and polarized cell expansion in *Arabidopsis thaliana* [corrected]. Development **130:** 4011–4024.

Grosskortenhaus, R., and Sprenger, F. (2002). Rca1 inhibits APC-Cdh1(Fzr) and is required to prevent cyclin degradation in G2. Dev. Cell **2:** 29–40.

Haga, N., Kato, K., Murase, M., Araki, S., Kubo, M., Demura, T., Suzuki, K., Müller, I., Voss, U., Jürgens, G., and Ito, M. (2007). R1R2R3-Myb proteins positively regulate cytokinesis through activation of *KNOLLE* transcription in *Arabidopsis thaliana*. Development **134:** 1101–1110.

Haga, N., Kobayashi, K., Suzuki, T., Maeo, K., Kubo, M., Ohtani, M., Mitsuda, N., Demura, T., Nakamura, K., Jürgens, G., and Ito, M. (2011). Mutations in *MYB3R1* and *MYB3R4* cause pleiotropic developmental defects and preferential down-regulation of multiple G2/M-specific genes in Arabidopsis. Plant Physiol. **157:** 706–717.

Hajdukiewicz, P., Svab, Z., and Maliga, P. (1994). The small, versatile pPZP family of Agrobacterium binary vectors for plant transformation. Plant Mol. Biol. **25:** 989–994.

Hara, K., Yokoo, T., Kajita, R., Onishi, T., Yahata, S., Peterson, K.M., Torii, K.U., and Kakimoto, T. (2009). Epidermal cell density is autoregulated via a secretory peptide, EPIDERMAL PATTERNING FACTOR 2 in *Arabidopsis* leaves. Plant Cell Physiol. **50:** 1019–1031.

Hase, Y., Trung, K.H., Matsunaga, T., and Tanaka, A. (2006). A mutation in the uvi4 gene promotes progression of endo-reduplication and confers increased tolerance towards ultraviolet B light. Plant J. **46:** 317–326.

Hemerly, A.S., Ferreira, P., de Almeida Engler, J., Van Montagu, M., Engler, G., and Inzé, D. (1993). *cdc2a* expression in *Arabidopsis* is linked with competence for cell division. Plant Cell **5:** 1711–1723.

Imai, K.K., Ohashi, Y., Tsuge, T., Yoshizumi, T., Matsui, M., Oka, A., and Aoyama, T. (2006). The A-type cyclin CYCA2;3 is a key regulator of ploidy levels in *Arabidopsis* endoreduplication. Plant Cell **18:** 382–396.

Inzé, D., and De Veylder, L. (2006). Cell cycle regulation in plant development. Annu. Rev. Genet. **40:** 77–105.

Jürgens, G. (2005). Plant cytokinesis: Fission by fusion. Trends Cell Biol. **15:** 277–283.

Kosetsu, K., Matsunaga, S., Nakagami, H., Colcombet, J., Sasabe, M., Soyano, T., Takahashi, Y., Hirt, H., and Machida, Y. (2010). The MAP kinase MPK4 is required for cytokinesis in *Arabidopsis thaliana*. Plant Cell **22:** 3778–3790.

Kubo, M., Udagawa, M., Nishikubo, N., Horiguchi, G., Yamaguchi, M., Ito, J., Mimura, T., Fukuda, H., and Demura, T. (2005). Transcription switches for protoxylem and metaxylem vessel formation. Genes Dev. **19:** 1855–1860.

Kevei, Z., Baloban, M., Da Ines, O., Tiricz, H., Kroll, A., Regulski, K., Mergaert, P., and Kondorosi, E. (2011). Conserved CDC20 cell cycle functions are carried out by two of the five isoforms in *Arabidopsis thaliana*. PLoS ONE **6:** e20618.

Kurihara, D., Matsunaga, S., Uchiyama, S., and Fukui, K. (2008). Live cell imaging reveals plant aurora kinase has dual roles during mitosis. Plant Cell Physiol. **49:** 1256–1261.

Kuromori, T., Hirayama, T., Kiyosue, Y., Takabe, H., Mizukado, S., Sakurai, T., Akiyama, K., Kamiya, A., Ito, T., and Shinozaki, K. (2004). A collection of 11 800 single-copy *Ds* transposon insertion lines in Arabidopsis. Plant J. **37:** 897–905.

Lammens, T., Boudolf, V., Kheibarshekan, L., Zalmas, L.P., Gaamouche, T., Maes, S., Vanstraelen, M., Kondorosi, E., La Thangue, N.B., Govaerts, W., Inzé, D., and De Veylder, L. (2008). Atypical E2F activity restrains APC/CCCS52A2 function obligatory for endocycle onset. Proc. Natl. Acad. Sci. USA **105:** 14721–14726.

Larson-Rabin, Z., Li, Z., Masson, P.H., and Day, C.D. (2009). FZR2/CCS52A1 expression is a determinant of endoreduplication and cell expansion in Arabidopsis. Plant Physiol. **149:** 874–884.

Lee, H.O., Davidson, J.M., and Duronio, R.J. (2009). Endoreplication: Polyploidy with purpose. Genes Dev. **23:** 2461–2477.

Levan, A. (1938). The effect of colchicine on root mitoses in Allium. Hereditas **24:** 471–486.

Lilly, M.A., and Duronio, R.J. (2005). New insights into cell cycle control from the Drosophila endocycle. Oncogene **24:** 2765–2775.

Machida, Y.J., and Dutta, A. (2007). The APC/C inhibitor, Emi1, is essential for prevention of rereplication. Genes Dev. **21:** 184–194.

Madgwick, S., Hansen, D.V., Levasseur, M., Jackson, P.K., and Jones, K.T. (2006). Mouse Emi2 is required to enter meiosis II by reestablishing cyclin B1 during interkinesis. J. Cell Biol. **174:** 791–801.

Marrocco, K., Bergdoll, M., Achard, P., Criqui, M.C., and Genschik, P. (2010). Selective proteolysis sets the tempo of the cell cycle. Curr. Opin. Plant Biol. **13:** 631–639.

Marrocco, K., Thomann, A., Parmentier, Y., Genschik, P., and Criqui, M.C. (2009). The APC/C E3 ligase remains active in most post-mitotic Arabidopsis cells and is required for proper vasculature development and organization. Development **136:** 1475–1485.

Nadeau, J.A. (2009). Stomatal development: New signals and fate determinants. Curr. Opin. Plant Biol. **12:** 29–35.

Nadeau, J.A., and Sack, F.D. (2002). Control of stomatal distribution on the Arabidopsis leaf surface. Science **296:** 1697–1700.

Nagl, W. (1978). Endopolyploidy and Polyteny in Differentiation and Evolution. (Amsterdam: North-Holland Publishing Company).

Nakamura, M., Naoi, K., Shoji, T., and Hashimoto, T. (2004). Low concentrations of propyzamide and oryzalin alter microtubule dynamics in Arabidopsis epidermal cells. Plant Cell Physiol. **45:** 1330–1334.

Nakamura, R.L., McKendree, W.L., Jr., Hirsch, R.E., Sedbrook, J.C., Gaber, R.F., and Sussman, M.R. (1995). Expression of an *Arabidopsis* potassium channel gene in guard cells. Plant Physiol. **109:** 371–374.

Narbonne-Reveau, K., Senger, S., Pal, M., Herr, A., Richardson, H.E., Asano, M., Deak, P., and Lilly, M.A. (2008). APC/CFzr/Cdh1 promotes cell cycle progression during the *Drosophila* endocycle. Development **135:** 1451–1461.

Ohashi-Ito, K., and Bergmann, D.C. (2006). *Arabidopsis* FAMA controls the final proliferation/differentiation switch during stomatal development. Plant Cell **18:** 2493–2505.

Perazza, D., Herzog, M., Hülskamp, M., Brown, S., Dorne, A.M., and Bonneville, J.M. (1999). Trichome cell growth in *Arabidopsis thaliana* can be derepressed by mutations in at least five genes. Genetics **152:** 461–476.

Pesin, J.A., and Orr-Weaver, T.L. (2008). Regulation of APC/C activators in mitosis and meiosis. Annu. Rev. Cell Dev. Biol. **24:** 475–499.

Peters, J.M. (2006). The anaphase promoting complex/cyclosome: a machine designed to destroy. Nat. Rev. Mol. Cell Biol. **7:** 644–656.

Pillitteri, L.J., Sloan, D.B., Bogenschutz, N.L., and Torii, K.U. (2007). Termination of asymmetric cell division and differentiation of stomata. Nature **445:** 501–505.

Saze, H., and Kakutani, T. (2007). Heritable epigenetic mutation of a transposon-flanked Arabidopsis gene due to lack of the chromatin-remodeling factor DDM1. EMBO J. **26:** 3641–3652.

Semiarti, E., Ueno, Y., Tsukaya, H., Iwakawa, H., Machida, C., and Machida, Y. (2001). The *ASYMMETRIC LEAVES2* gene of *Arabidopsis thaliana* regulates formation of a symmetric lamina, establishment of venation and repression of meristem-related homeobox genes in leaves. Development **128:** 1771–1783.

Soyano, T., Nishihama, R., Morikiyo, K., Ishikawa, M., and Machida, Y. (2003). NQK1/NtMEK1 is a MAPKK that acts in the NPK1 MAPKKK-mediated MAPK cascade and is required for plant cytokinesis. Genes Dev. **17:** 1055–1067.

Ten Hove, C.A., and Heidstra, R. (2008). Who begets whom? Plant cell fate determination by asymmetric cell division. Curr. Opin. Plant Biol. **11:** 34–41.

Van Leene, J., et al. (2010). Targeted interactomics reveals a complex core cell cycle machinery in *Arabidopsis thaliana*. Mol. Syst. Biol. **6:** 397.

Vanstraelen, M., Baloban, M., Da Ines, O., Cultrone, A., Lammens, T., Boudolf, V., Brown, S.C., De Veylder, L., Mergaert, P., and Kondorosi, E. (2009). APC/C-CCS52A complexes control meristem maintenance in the Arabidopsis root. Proc. Natl. Acad. Sci. USA **106:** 11806–11811.

Weingartner, M., Criqui, M.C., Mészáros, T., Binarova, P., Schmit, A.C., Helfer, A., Derevier, A., Erhardt, M., Bögre, L., and Genschik, P. (2004). Expression of a nondegradable cyclin B1 affects plant development and leads to endomitosis by inhibiting the formation of a phragmoplast. Plant Cell **16:** 643–657.

Weiss, H., and Maluszynska, J. (2001). Molecular cytogenetic analysis of polyploidization in the anther tapetum of diploid and autotetraploid *Arabidopsis thaliana* plants. Ann. Bot. (Lond.) **87:** 729–735.

Wu, G., Glickstein, S., Liu, W., Fujita, T., Li, W., Yang, Q., Duvoisin, R., and Wan, Y. (2007). The anaphase-promoting complex coordinates initiation of lens differentiation. Mol. Biol. Cell **18:** 1018–1029.

Yang, Y., Kim, A.H., Yamada, T., Wu, B., Bilimoria, P.M., Ikeuchi, Y., de la Iglesia, N., Shen, J., and Bonni, A. (2009). A Cdc20-APC ubiquitin signaling pathway regulates presynaptic differentiation. Science **326:** 575–578.

Zhang, Y., Wang, Z., Liu, D.X., Pagano, M., and Ravid, K. (1998). Ubiquitin-dependent degradation of cyclin B is accelerated in polyploid megakaryocytes. J. Biol. Chem. **273:** 1387–1392.

Zielke, N., Querings, S., Rottig, C., Lehner, C., and Sprenger, F. (2008). The anaphase-promoting complex/cyclosome (APC/C) is required for rereplication control in endoreplication cycles. Genes Dev. **22:** 1690–1703.